IET Microwaves, Antennas & Propagation

Research Article

IET Journals
The Institution of Engineering and Technology

Decoupling between ground radiation antennas with ground-coupled loop-type isolator for WLAN applications

ISSN 1751-8725
Received on 6th April 2015
Revised on 14th December 2015
Accepted on 18th December 2015
doi: 10.1049/iet-map.2015.0562
www.ietdl.org

Longyue Qu, Rui Zhang, Hyeongdong Kim ✉

Department of Electronic Engineering, Hanyang University, 222 Wangsimni-ro, Seongdong-gu, Seoul, Republic of Korea
✉ *E-mail: hdkim@hanyang.ac.kr*

Abstract: A compact and easy to fabricate decoupling method is proposed to yield high isolation for the multiple-input and multiple-output (MIMO) ground radiation antenna (GradiAnt) system. The proposed MIMO antenna system is comprised of two symmetrical, closely spaced, loop-type (GradiAnts) with a ground-coupled loop-type isolator inserted between them. The isolator can be seen as a series resonant circuit which is connected with lumped components to control decoupling. In the proposed MIMO GradiAnt system, a coupling null is induced due to the ground-coupled isolator, which effectively can be used for isolation enhancement between two GradiAnts. Within WLAN band, a minimum 14 dB isolation with a peak value of 42 dB at 2.42 GHz is achieved. In this manuscript, the decoupling principle and controlling mechanisms are first explained, then the antenna performances and tuning mechanisms are discussed in detail. The simulation and the measurement of the MIMO antenna, including the scattering parameters, efficiency, radiation patterns, peak gains and envelope correlation coefficients are conducted to verify the performance of the proposed MIMO system.

1 Introduction

In wireless communications, multiple-input and multiple-output (MIMO) antenna systems are able to increase system capacity by their multiple isolated antennas, which simultaneously transmit and receive signals, and thus can be of great use in 4G communications [1]. However, the MIMO antennas often suffer from strong mutual coupling due to small ground size and compact located antennas, which can degrade the bandwidth and radiation efficiency as well as correlation, leading to reduced system capacity. Therefore, reducing mutual coupling or enhancing the port isolation is an important requirement for strongly coupled MIMO antennas.

There have been many studies on increasing the port isolation in MIMO antennas and most fall into one of two strategies: the addition of parasitic elements [2–14] and the use of decoupling networks [15–19]. The former is typically carried out by using $\lambda/4$-length resonators such as monopoles [2, 3], slits [3], stubs [4, 5], slots [6, 7] and $\lambda/2$-length resonators such as slots [7], dipoles [8–10], digits [11], strips [12, 13], novel structures such as metamaterial structures [14], magnetic band gap (EBG) structures [15] in between aggressive antennas. In the latter technique, decoupling networks using lumped elements are analysed in [16, 17], in a similar way neutralisation lines are adopted in [18–20].

For the technique of parasitic elements, the above studies usually adopted parasitic elements with a specific shape to achieve isolation enhancement between antenna elements such as dipoles, monopoles, IFAs or PIFAs. In this paper, we proposed an alternative way of ground-coupled loop-type isolator with loaded components, which is suitable for decoupling ground radiation antennas (GradiAnt) where the decoupling effect is mainly achieved through the coupling between the ground plane and ground-coupled isolator. The proposed isolator operates as a series resonant circuit with controllable lumped components which can be used for resonant frequency adjustment and size reduction as well as coupling adjustment with the ground plane. The proposed isolator structure is able to solve practical problems, especially in small size PCBs where little space is provided, with ease of fabrication, tune-ability and flexibility of shape as well as location. The GradiAnt is a small loop-type antenna which excites the ground plane as a dipole-type radiator [21, 22]. The proposed MIMO system comprises two GradiAnts and a ground-coupled loop-type isolator inserted between them. Each antenna is placed symmetrically along the edge of the long side of the PCB ground plane and operates at 2.4 GHz WLAN band. The proposed MIMO GradiAnt system with the proposed ground-coupled isolator is demonstrated in Section 2 and the theoretical analysis is explained in Section 3. In Section 4, the simulated parametric studies are analysed. The performance of the proposed MIMO GradiAnt system is measured using Agilent 8753ES network analysers and a 6 m × 3 m 3D CTIA OTA chamber and discussed in Section 5.

2 Design of MIMO GradiAnt system

The proposed MIMO GradiAnt system for 2.4 GHz WLAN application is shown in Fig. 1. The ground plane of 100 mm × 50 mm is printed on a low-cost FR4 substrate with thickness of 1 mm and dielectric constant $\epsilon_r = 4.4$. The GradiAnts are located at 22 mm from either edge on the top side of the PCB considering good radiation instead of mutual coupling. Each GradiAnt is identical and mirror-symmetric, with a ground clearance of 8 mm × 5 mm. A series capacitor, C_R, is employed for resonant frequency adjustment and excited by a feeding loop with dimensions 4.5 mm × 2.5 mm. A series capacitor C_F is used in the feeding loop for impedance matching. The edge-to-edge separation of the two GradiAnts is 40 mm (0.32 λ). It has demonstrated that the each GradiAnt will excite the long side of the ground plane as a λ-length radiator, so that strong mutual coupling will be generated for the same radiation pattern. Therefore, a strong coupled current would be induced from one antenna port to another, and the average isolation between the two GradiAnts turns to be 10 dB.

To reduce the mutual coupling and enhance the isolation between the GradiAnts, a 5 mm × w mm loop-type isolator is inserted, as shown in Fig. 1. The proposed isolator is loaded with series lumped components, which can be capacitors, inductors or resistors so that it is controllable for resonant frequency and decoupling effect. The isolator can be seen as a source-free GradiAnt, which will strongly couple with the ground plane and the dipole-type currents generated by the GradiAnts. Therefore, by choosing approximate components, the optimal decoupling effect can be achieved. In the optimised

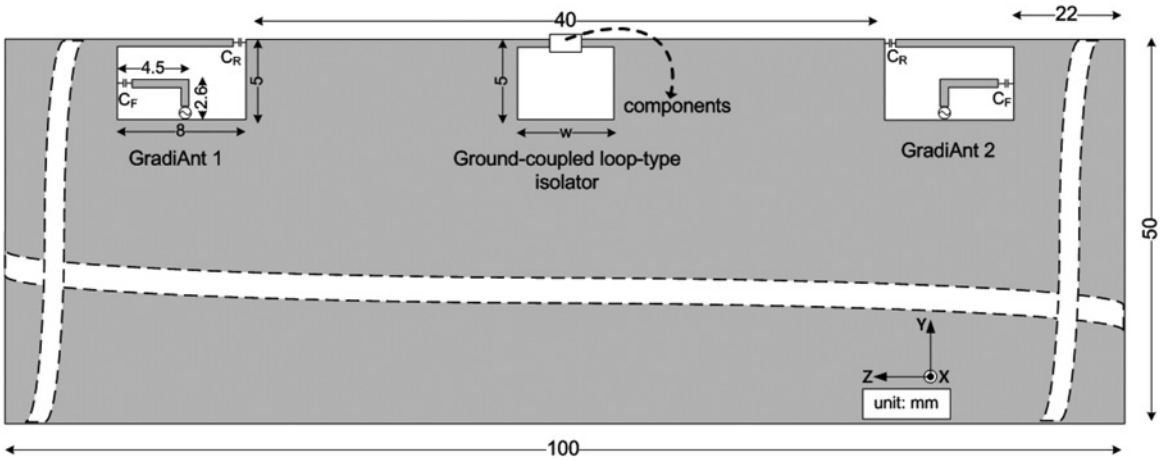

Fig. 1 *Geometry of the proposed MIMO GradiAnt system with the ground-coupled loop-type isolator*

GradiAnt MIMO system design, the 5 mm × 6 mm ground-coupled loop-type isolator with loaded capacitor of 0.79 pF is designed by simulation and tested in measurements.

The simulated scattering parameters of the MIMO GradiAnt system with and without the ground-coupled isolator are shown in Fig. 2. The MIMO GradiAnts system without the ground-coupled isolator is assigned to be the reference design with an average 10 dB isolation in the operating band. In the proposed MIMO GradiAnt system, a coupling null is introduced into the S_{12} curve due to the isolator, so that the isolation between GradiAnts is over 14 dB in the entire operating band with a peak value of 42 dB at 2.42 GHz, representing great isolation enhancement by inserting the ground-coupled isolator. Since the proposed antenna structures are symmetrical, the scattering parameters of antenna 1 and antenna 2 are nearly the same; thus, both S_{11} and S_{22} are represented by a single curve. In the S_{11}/S_{22} curve, a 10 dB return loss bandwidth of 250 MHz (from 2.38 to 2.63 GHz) is obtained, covering all the 2.4 G WLAN band; and the 10 dB return loss bandwidth without the isolator is 250 MHz (from 2.32 to 2.57 GHz). Even a little shift in the resonant frequency of the antenna is generated due to the isolator, there is no much effect on the antenna performance.

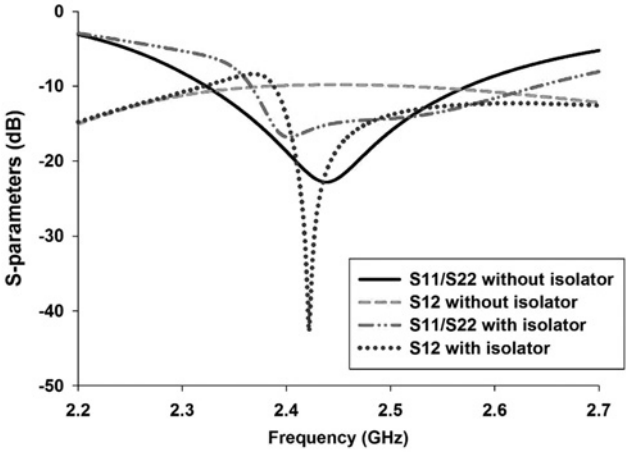

Fig. 2 *Simulated S-parameters of the MIMO GradiAnt system with and without the proposed isolator*

3 Theoretical analysis

The proposed MIMO GradiAnt system design can be explained by the three-port microwave network and decoupling theorem; the ground-coupled isolator acts as a third port (port 3) between the two WLAN GradiAnts (port 1 and port 2). Then the scattering matrix, or [***S***] matrix of the three-port microwave network is determined by (1), as follows

$$\begin{bmatrix} V_1^- \\ V_2^- \\ V_3^- \end{bmatrix} = \begin{bmatrix} S_{11} & S_{12} & S_{13} \\ S_{21} & S_{22} & S_{23} \\ S_{31} & S_{32} & S_{33} \end{bmatrix} \begin{bmatrix} V_1^+ \\ V_2^+ \\ V_3^+ \end{bmatrix} \quad (1)$$

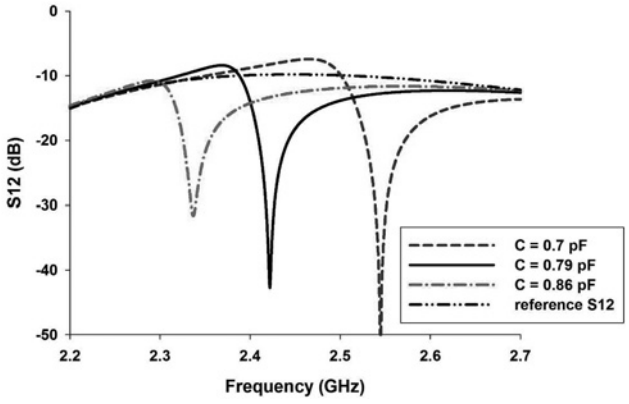

Fig. 3 *Simulated parametric study: S_{12} against frequency for various values of the capacitor C*

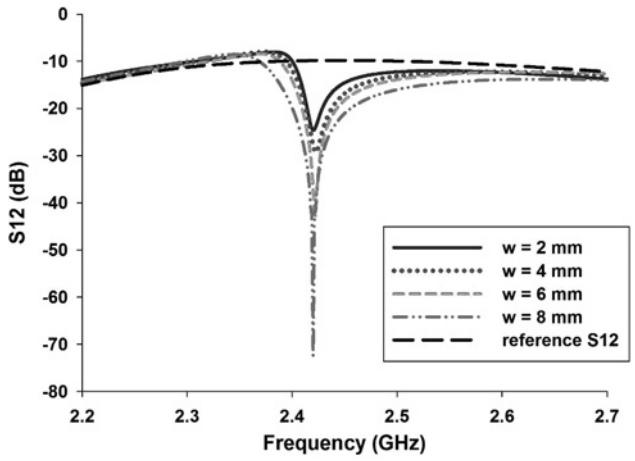

Fig. 4 *Simulated parametric study: S_{12} against frequency for various widths of the isolator*

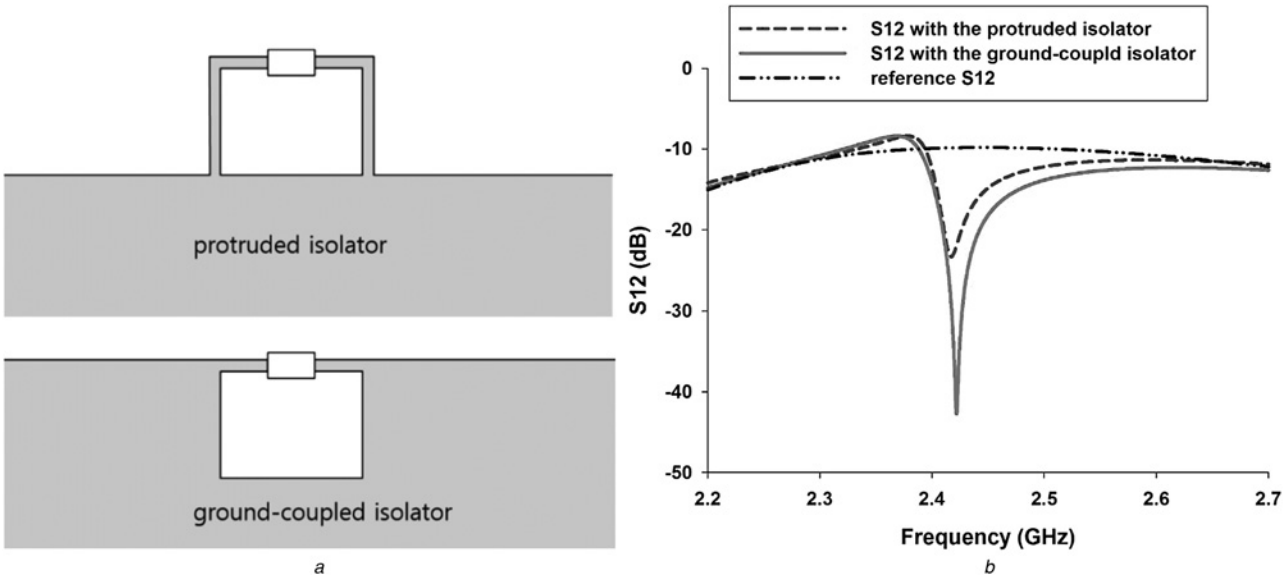

Fig. 5 *Comparison of the protruded isolator and the proposed ground-coupled isolator*

a Configuration of the protruded isolator and the proposed ground-coupled isolator
b Simulated S_{12} with the protruded isolator and the proposed ground-coupled isolator

where V_n^+ and V_n^- are the amplitudes of the voltage wave incident and that reflected from port n, respectively. The termination condition for port 3 (ground-coupled isolator) implies the following equation

$$\Gamma = \frac{V_3^+}{V_3^-} = \frac{Z_L - Z_0}{Z_L + Z_0} \tag{2}$$

where Γ is the reflection coefficient at port 3, and Z_L and Z_0 are the load impedance and the characteristic impedance.

From (2) and (1), we calculate

$$S'_{12} = S_{12} + \frac{S_{13}S_{23}\Gamma}{1 - \Gamma S_{33}} \tag{3}$$

where S'_{12} and S_{12} are the transmission coefficients from port 1 to port 2 with and without the ground-coupled isolator, respectively. This equation can be represented as the decoupling theorem [23]. Accordingly, by adjusting the relevant parameters in the latter part of the above equation, the coupled ports (port 1 and port 2) can be decoupled, preventing the flow of power from port 1 to port 2, or from port 2 to port 1. The decoupling effect depends on the coupling between the ground-coupled isolator and GradiAnt (S_{13} and S_{23}), and on the property of the ground-coupled isolator itself (Z_L).

As mentioned above, the GradiAnt is a small loop-type antenna, which can excite the ground plane as a dipole-type radiator. According to the reaction concept and the theory of characteristic modes for conducting bodies [24, 25], the coupling between the ground plane and the GradiAnt can be represented by the modal excitation coefficient [25] which is expressed as

$$V_n^i = -\iiint_\tau \left(\bar{H}_{\text{ground}} \cdot \bar{M}^{\text{GradiAnt}}\right) \mathrm{d}\tau \tag{4}$$

where $\bar{H}_{\text{ground}}$ denotes the magnetic field produced by the characteristic currents on the ground plane [25], and $\bar{M}^{\text{GradiAnt}}$ is the impressed magnetic current produced by the GradiAnt. Therefore, the loop-type current mode $\bar{M}^{\text{GradiAnt}}$ can react with the characteristic magnetic field $\bar{H}_{\text{ground}}$ of the ground plane, inducing as a dipole-type current mode on the ground plane. In this sense, the ground-coupled loop-type isolator works by the same principle

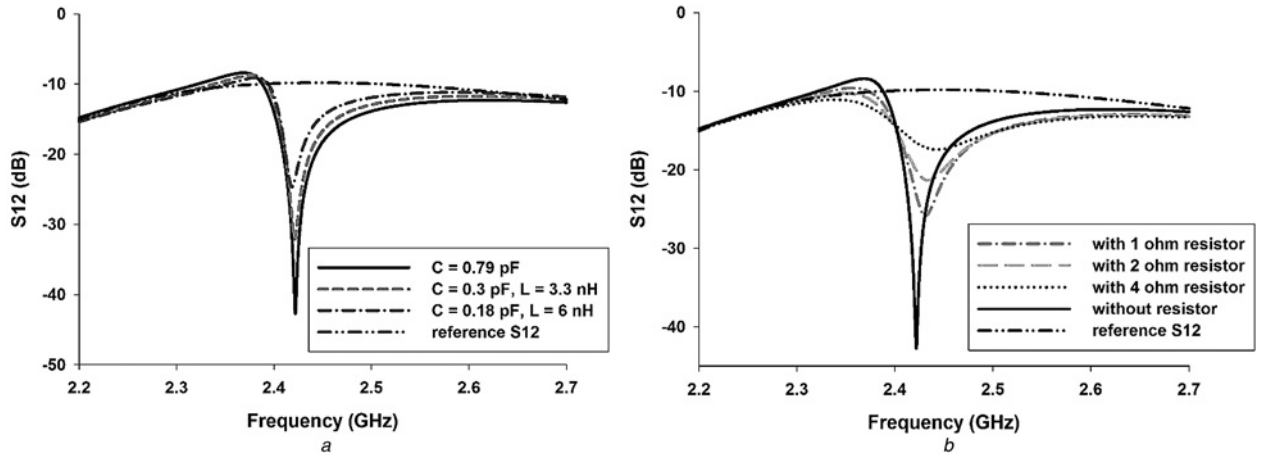

Fig. 6 *Simulated parametric study: S_{12} against frequency for various components*

a Capacitors and inductors
b Resistors

IET Microw. Antennas Propag., 2016, Vol. 10, Iss. 5, pp. 546–552

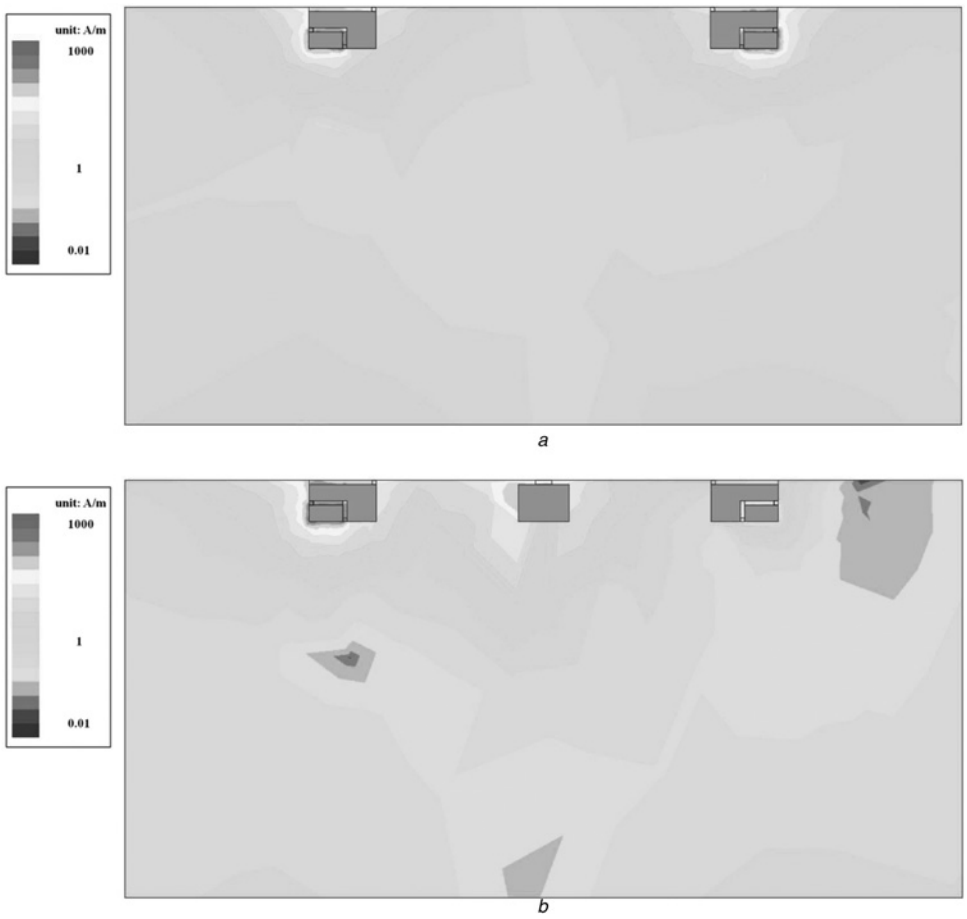

Fig. 7 *Surface current distributions upon 2.45-GHz excitation of antenna 1*

a Without the proposed isolator
b With the proposed isolator

as the GradiAnt does, so that the ground-coupled isolator and GradiAnts can couple with each other through the ground plane. Therefore, the decoupling effect of the ground-coupled isolator can be enhanced by the coupling with the ground plane and can be adjusted by the components.

4 Tuning mechanisms and parametric studies

On the tuning mechanisms of the ground-coupled isolator, the first problem is the frequency controlling technique of the coupling null.

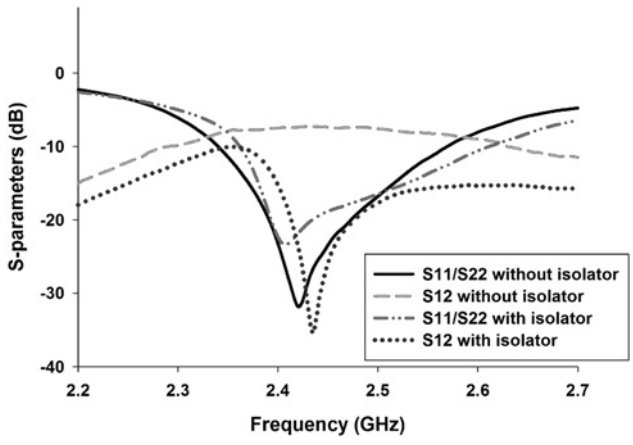

Fig. 8 *Measured scattering parameters of the GradiAnt MIMO system with and without the ground-coupled isolator*

In the proposed MIMO GradiAnt system, the location of the coupling null is always around and is dependent on the resonant frequency of the isolator; thus, the size of the isolator and the loaded lumped components will determine the resonant frequency of the decoupling resonator, further determining the location of the coupling null. Meanwhile, by adjusting the components, the location of the coupling null can be easily controlled without changing the size of the isolator. As shown in Fig. 3, the coupling null is shifted from 2.54 to 2.33 GHz when the capacitor increases from 0.70 to 0.86 pF, indicating that the coupling null shifts simultaneously with the resonant frequency of the decoupling resonator. By trying several values of the lumped elements, the peak of the coupling null is easily adjusted at 2.42 GHz for the demand of WLAN applications when the capacitor is set to be 0.79 pF, and the minimum isolation over the operating band is 14 dB.

Another important parameter to be studied is the decoupling effect of the ground-coupled isolator, that is, bandwidth and magnitude of isolation. The decoupling of the isolator, coupled with the ground plane, can be improved by enhancing the coupling with the ground plane. It can be determined by the parameters of the ground-coupled isolator. The idea is different from other decoupling structures. To obtain the optimum size of the isolator on the decoupling effect, various widths 'w' of the isolator are analysed as shown in Fig. 4. The coupling null gets deeper and wider as w increases due to stronger coupling with the ground plane which cancels out the mutual coupling of MIMO antennas according to the decoupling theorem and reaction concept demonstrated in Section 3. Note that, to maintain the location of the coupling null, the value of the loaded capacitor must be adjusted accordingly as the size of the isolator changes. Consequently, the proposed ground-coupled isolator can have stronger coupling with the ground plane resulting in larger

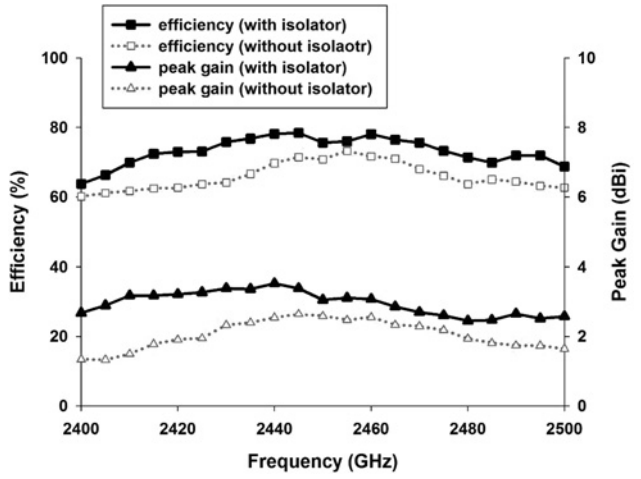

Fig. 9 *Measured radiation efficiency of the proposed MIMO antenna*

decoupling effect. In this sense, the isolator can be constructed in any shape as long as it effectively couples with the ground plane.

To demonstrate the novelty of the proposed ground-coupled isolator, the configurations of the protruded isolator and the proposed ground-coupled isolator, having the same size, are demonstrated and compared in Fig. 5*a*. The ground-coupled isolator is inside the ground plane and thus has stronger coupling with the ground plane than the protruded isolator. Note that the protruded isolator is connected with a 1 pF capacitor and occupies the same size as that of ground-coupled isolator. As we can see in Fig. 5*b*, the ground-coupled isolator achieves better decoupling effect on the level of the coupling null at the WLAN band. Therefore, the ground-coupled isolator can be more effective through the coupling with the ground plane for isolation enhancement in proposed MIMO GradiAnt system.

As stated above, the ground-coupled isolator can be modelled as a series RLC resonator. Therefore, the properties of the ground-coupled isolator including the capacitance, inductance and resistance will determine the coupling with the ground plane that in turn will determine the decoupling effect. Different lumped

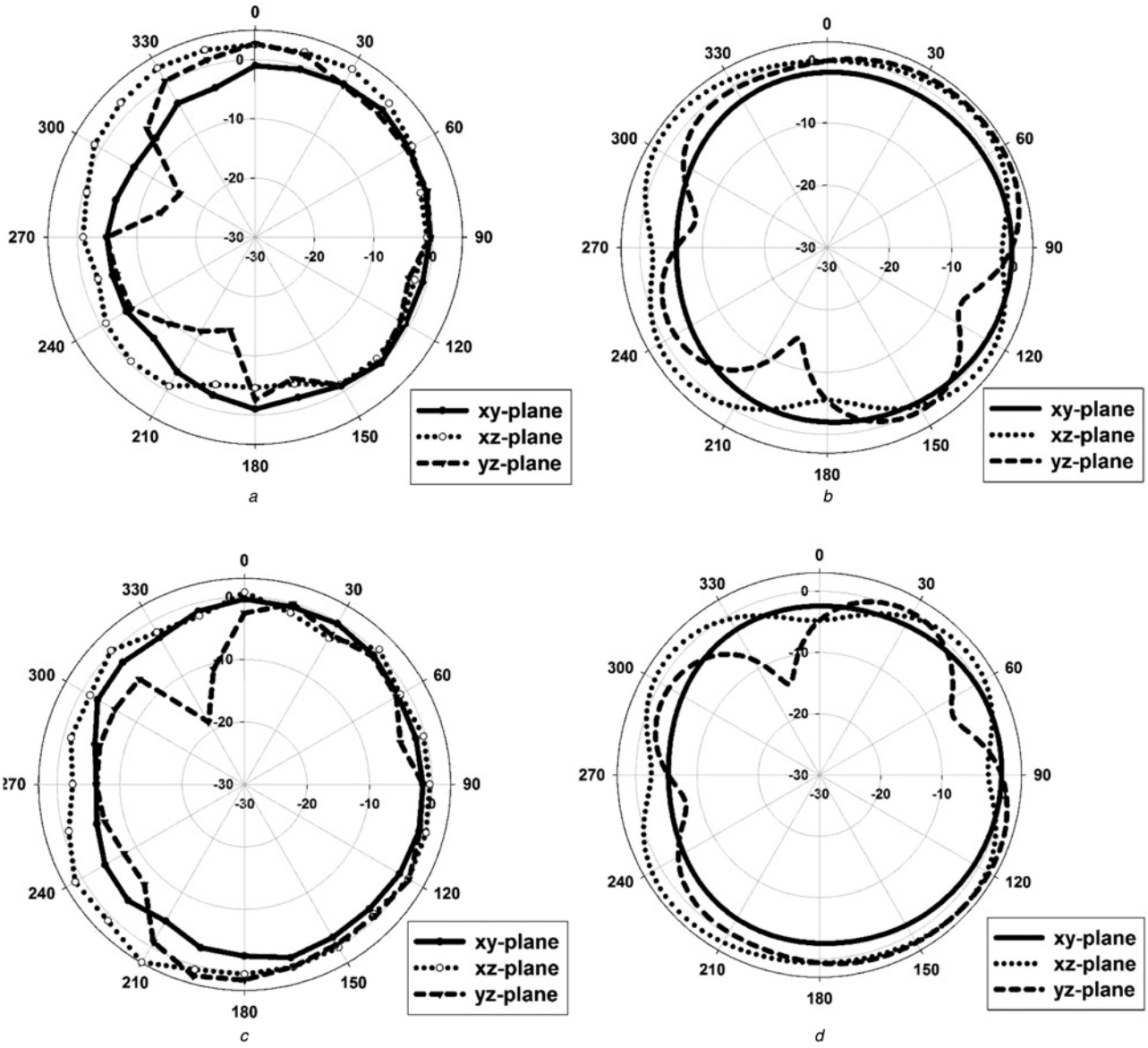

Fig. 10 *Measured and simulated radiation patterns at 2.45 GHz with the proposed ground-coupled isolator*

a Measured radiation patterns of port 1
b Simulated radiation patterns of port 1
c Measured radiation patterns of port 2
d Simulated radiation patterns of port 2

IET Microw. Antennas Propag., 2016, Vol. 10, Iss. 5, pp. 546–552

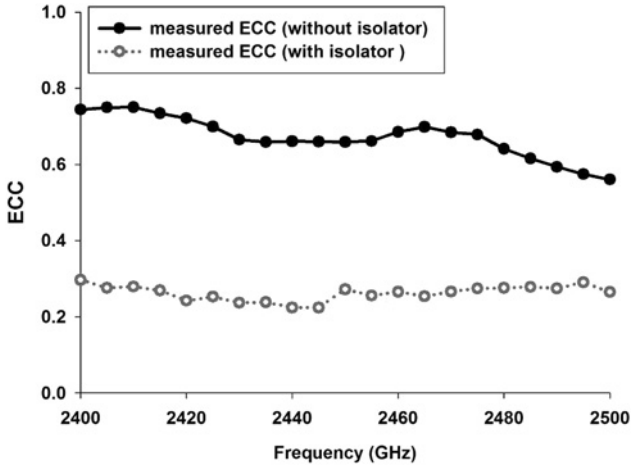

Fig. 11 *Measured ECC of the MIMO GradiAnt antenna with and without the ground-coupled isolator*

components are analysed to study the decoupling effect, which is demonstrated in Fig. 6*a*. This is conducted by adjusting the ratio of the series inductor and capacitor while maintaining the coupling null at 2.42 GHz. The decoupling effect of the coupling null degrades as the ratio of inductance and capacitance increases (increasing the inductor L from 0 to 6 nH while decreasing the capacitor C from 0.79 to 0.18 pF). Furthermore, the effect of the resistor is also studied by inserting a resistor in the proposed ground-coupled isolator in series with the capacitor. In Fig. 6*b*, added resistance leads to wider coupling null but the isolation level is also degraded as the resistance increases. In case of different applications the components can be tuned in order to adjust the coupling between the isolator and the ground plane.

To better understand the decoupling effect of the ground-coupled isolator, the surface current distributions on the GradiAnts with and without the proposed isolator are provided in Fig. 7. This is done by exciting port 1 at 2.45 GHz while port 2 is terminated with a 50-Ω load. For the GradiAnts without the proposed isolator, a direct and strong coupling current is induced from port 1 to port 2, as shown in Fig. 7*a*. While in Fig. 7*b*, the proposed ground-coupled isolator works as a new coupling path from antenna 1 to antenna 2 cancelling out the mutual coupling between antenna elements, so that we can see the coupling current from port 1 is directed to the ground-coupled isolator instead of port 2. Note that stronger induced currents into port 2 means strong mutual coupling between port 1 and port 2. Therefore, the proposed ground-coupled isolator can effectively reduce the mutual coupling between GradiAnts, which is consistent with the scattering parameters demonstrated above.

5 Measurement results and performance of MIMO GradiAnt system

The measurement data are conducted to verify the MIMO performance of the proposed MIMO GradiAnt system. In Fig. 8, the measured scattering parameters with and without the proposed ground-coupled isolator are shown. The measured isolation between two GradiAnts with the proposed ground-coupled loop-type isolator is above 17 dB in the WLAN operating band with a peak of 37 dB at 2.42 GHz and that without the proposed isolator is 10 dB in average. The measurement data confirms that the addition of the ground-coupled isolator indeed enhanced the mutual coupling without much effect on the antenna characteristics, which agrees well with the simulated data.

Then the total radiation efficiency of the GradiAnt is measured from 2.4 to 2.5 GHz by exciting port 1 while terminating port 2 with a 50-Ω load. In Fig. 9, the measured radiation efficiency ranges from 62 to 76% over the whole frequency range, averaging 71%, which is suitable for MIMO applications. While the average efficiency of the reference design without isolator is measured to be 64%. On the other hand, the measured peak gains with and without isolator are also plotted in Fig. 9. It can be observed that the design with the proposed ground-coupled isolator gives improved gain.

To analyse the diversity performance of the proposed MIMO GradiAnt system, the radiation patterns of the MIMO GradiAnts with the proposed ground-coupled isolator are measured in a 6 m × 3 m 3D CTIA OTA anechoic chamber. Fig. 10 displays the simulated and measured radiation patterns at 2.45 GHz (the measured port is excited while another port is terminated with a 50-Ω load). The simulated and measured radiation patterns are consistent for both antennas, as we can see, and each antenna produces omni-directional patterns on the *xy*-plane. Furthermore, from the measured radiation patterns of MIMO GradiAnts, the envelope correlation coefficients (ECC) ρ_e for the proposed two-antenna system is calculated from (5) [26], as

$$\rho_e = \frac{\left|\iint_{4\pi}\left[\boldsymbol{F}_1(\theta,\phi)\boldsymbol{F}_2(\theta,\phi)\right]\mathrm{d}\Omega\right|^2}{\iint_{4\pi}\left|\boldsymbol{F}_1(\theta,\phi)\right|^2\mathrm{d}\Omega\iint_{4\pi}\left|\boldsymbol{F}_2(\theta,\phi)\right|^2\mathrm{d}\Omega} \tag{5}$$

where $F_i(\theta, \phi)$ is the field radiation pattern of the antenna system when port i is excited. As plotted in Fig. 11, all the values are maintained below 0.3, much lower than that of without isolator which is above 0.6. This implies that the diversity performance is also improved with the ground-coupled isolator. In mobile communications, the ECC of the MIMO system should be lower than 0.5, which is acceptable for diversity considerations [26]. Therefore, the proposed MIMO GradiAnt system satisfies the conditions for diversity performance and is suitable for MIMO applications.

6 Conclusion

An easy to fabricate and effective method is proposed to enhance the isolation between two GradiAnts for 2.4 GHz WLAN applications by inserting a ground-coupled loop-type isolator. The proposed ground-coupled isolator is a 5×6 mm^2 rectangular loop in series with lumped components, which decouples GradiAnts by coupling with the ground plane, so that the isolator can be made compact, shape-free and tunable. In measurements, an isolation over 17 dB in the WLAN operating band with a peak of 37 dB at 2.42 GHz is achieved and high efficiency and peak gain are also obtained as compared with the reference MIMO antenna. The measured ECC is under 0.3, which means high diversity performance and satisfies the conditions for MIMO application in mobile system.

7 Acknowledgments

This work was supported by the National Research Foundation of Korea (NRF) grant funded by the Korea government (MSIP) (grant no. 2015R1A2A1A15055109).

8 References

1 Garg, V.K.: 'wireless communications and networking' (Elsevier Publishing Company, 2008)
2 Khan, M.S., Shafique, M.F., Naqvi, A., *et al.*: 'A miniaturized dual-band MIMO antenna for WLAN applications', *IEEE Antennas Wirel. Propag. Lett.*, 2015, **14**, pp. 958–961
3 Li, J.-F., Chu, Q.-X., Huang, T.-G.: 'A compact wideband MIMO antenna with two novel bent slits', *IEEE Trans. Antennas Propag.*, 2012, **60**, (2), pp. 482–489
4 Liao, W.-J., Chang, S.-H., Yeh, J.-T., *et al.*: 'Compact dual-band WLAN diversity antennas on USB dongle platform', *IEEE Trans. Antennas Propag.*, 2014, **62**, (1), pp. 109–118
5 Toktas, A., Akdagli, A.: 'Wideband MIMO antenna with enhanced isolation for LTE, WiMAX and WLAN mobile handsets', *IET Electron. Lett.*, 2014, **50**, (10), pp. 723–724
6 Karaboikis, M., Soras, C., Tsachtsiris, G., *et al.*: 'Compact dual-printed inverted-F antenna diversity systems for portable wireless devices', *IEEE Antennas Wirel. Propag. Lett.*, 2004, **3**, (1), pp. 9–14

7 Saraereh, O.A., Panagamuwa, C.J., Vardaxoglou, J.C.: 'Low correlation multiple antenna system for mobile phone applications using novel decoupling slots in ground plane'. IEEE Antennas and Propagation Conf., Loughborough, England, November 2013, pp. 577–581
8 Lau, B.K., Andersen, J.B.: 'Simple and efficient decoupling of compact arrays with parasitic scatters', *IEEE Trans. Antennas Propag.*, 2012, **60**, (2), pp. 464–472
9 Li, Z., Du, Z., Takahashi, M., *et al*.: 'Reducing mutual coupling of MIMO antennas with parasitic elements for mobile terminals', *IEEE Trans. Antennas Propag.*, 2012, **60**, (2), pp. 473–481
10 Roshna, T.K., Deepak, U., Sajitha, V.R., *et al*.: 'A Compact UWB MIMO antenna with reflector to enhance isolation', *IEEE Trans. Antennas Propag.*, 2015, **63**, (4), pp. 1873–1877
11 Khan, M.S., Capobianco, A.-D., Najam, A.I., *et al*.: 'Compact ultra-wideband diversity antenna with a floating parasitic digitated decoupling structure', *IET Microw. Antennas Propag.*, 2014, **8**, (10), pp. 747–753
12 Lee, C.-H., Chen, S.-Y., Hsu, P.: 'Integrated dual planar inverted-F antenna with enhanced isolation', *IEEE Antennas Wirel. Propag. Lett.*, 2009, **8**, pp. 963–965
13 Khan, M.S., Capobianco, A.-D., Shafique, M.F., *et al*.: 'Isolation enhancement of a wideband MIMO antenna using floating parasitic elements', 2015, **57**, (7), pp. 1677–1682
14 Hsu, C.-C., Lin, K.-H., Su, H.-L.: 'Implementation of broadband isolator using metamaterial-inspired resonators and a T-shaped branch for MIMO antennas', *IEEE Trans. Antennas Propag.*, 2011, **59**, (10), pp. 3936–3939
15 Lei, Q., Zhao, F., Xiao, K., *et al*.: 'Transmit–receive isolation improvement of antenna arrays by using EBG structures', *IEEE Antennas Wirel. Propag. Lett.*, 2012, **11**, pp. 93–96
16 Tang, X., Mouthaan, K., Coetzee, J.C.: 'Tunable decoupling and matching network for diversity enhancement of closely spaced antennas', *IEEE Antennas Wirel. Propag. Lett.*, 2012, **11**, pp. 268–271
17 Chen, S.-C., Wang, Y.-S., Chung, S.-J.: 'A decoupling technique for increasing the port isolation between two strongly coupled antennas', *IEEE Trans. Antennas Propag.*, 2008, **56**, (12), pp. 3650–3658
18 Su, S.-W., Lee, C.-T., Chang, F.-S.: 'Printed MIMO-antenna system using neutralization-line technique for wireless USB-dongle applications', *IEEE Trans. Antennas Propag.*, 2012, **60**, (2), pp. 456–463
19 Diallo, A., Luxey, C., Le Thuc, P., *et al*.: 'Study and reduction of mutual coupling between two mobile phone PIFAs operating in the DCS1800 and UMTS bands', *IEEE Trans. Antennas Propag.*, 2006, **54**, (11), pp. 3063–3074
20 Chebihi, A., Luxey, C., Diallo, A., *et al*.: 'A novel isolation technique for closely spaced PIFAs for UMTS mobile phones', *IEEE Antennas Wirel. Propag. Lett.*, 2008, **7**, pp. 665–668
21 Cho, O., Choi, H., Kim, H.: 'Loop-type ground antenna using capacitor', *IET Electron. Lett.*, 2011, **47**, (1), pp. 11–12
22 Liu, Y., Lee, J., Kim, H.H., *et al*.: 'Ground radiation method using slot with coupling capacitors', *IET Electron. Lett.*, 2013, **49**, (7), pp. 447–448
23 Pozar, D.M.: 'Microwave engineering' (John Wiley & Sons, Inc., 2011, 4th edn.)
24 Harrington, R.F.: 'Time-harmonic electromagnetic fields' (Macgraw-Hill, New York, 1961)
25 Harrington, R.F., Mautz, J.R.: 'Theory of characteristic modes for conducting bodies', *IEEE Trans. Antennas Propag.*, 1971, **19**, (5), pp. 622–628
26 Vaughan, R.G., Andersen, J.B.: 'Antenna diversity in mobile communications', *IEEE Trans. Veh. Technol.*, 1987, **36**, (4), pp. 149–172